红外与激光工程
INFRARED AND LASER ENGINEERING
EI, SCOPUS, CSCD等收录期刊

距离漂移误差抑制获取Gm-APD激光雷达高精度三维像

徐璐　杨旭　吴龙　包晓安　张一嘉

Restrain range walk error of Gm-APD lidar to acquire high-precision 3D image

Xu Lu, Yang Xu, Wu Long, Bao Xiaoan, Zhang Yijia

在线阅读 View online: https://doi.org/10.3788/IRLA.20200218

Restrain range walk error of Gm-APD lidar to acquire high-precision 3D image

Xu Lu, Yang Xu, Wu Long*, Bao Xiaoan, Zhang Yijia

(School of Informatics, Zhejiang Sci-Tech University, Hangzhou 310018, China)

Abstract: Due to the first photon bias effect of Gm-APD, there exists range walk error in Gm-APD lidar, which will generate a distortion of depth image of the target. Two methods to restrain the range walk error were presented and verified by experiments. Signal restoration method was used to obtain signal photoelectron distribution histogram (SPDH) from the photon counting distribution histogram (PCDH). A sum of two Gaussian functions were used to fit the SPDH through, and the peak position of the curve was found to calculate the distance. The center-of-mass algorithm method on the SPDH was used to calculate the distance through the second method. The high-precision 3D depth-intensity merged images was caputured using the two methods by experiments with a 6 ns width laser pulse. The relative accuracy of intensity measurement of the two methods were both less than 3%. The signal restoration & Gaussian functions fitting method has range precision of 1.2 cm. The signal restoration & center-of-mass algorithm method has range precision of 0.6 cm.

Key words: lidar; photon counting; rang walk error; 3D imaging; Poisson statistics

CLC number: TN958.98 **Document code:** A **DOI:** 10.3788/IRLA.20200218

距离漂移误差抑制获取 Gm-APD 激光雷达高精度三维像

徐 璐, 杨 旭, 吴 龙*, 包晓安, 张一嘉

(浙江理工大学 信息学院, 浙江 杭州 310018)

摘 要: 由于 Gm-APD 存在第一光子偏移效应,Gm-APD 激光雷达存在距离漂移误差,并引起距离像的畸变。提出了两种抑制距离漂移误差的方法,并完成了实验验证。利用信号复原算法从光子计数分布图中复原了信号光电子数分布图。第一种方法采用双高斯函数对光电子数分布图进行拟合,并利用峰值位置计算距离。第二种方法采用质心算法对光电子数分布图进行加权计算并获取距离。采用 6 ns 脉冲宽度的激光,利用两种方法都获取了目标的高精度距离—强度三维融合像。两种方法的强度测量相对精度都小于 3%。信号复原&双高斯拟合寻峰法的测距精度为 1.2 cm。信号复原&质心算法的测距精度为 0.6 cm。

关键词: 激光雷达; 光子计数; 距离漂移误差; 三维成像; 泊松统计

收稿日期: 2020-06-02; **修订日期:** 2020-07-13

基金项目: 浙江省自然科学基金青年科学基金 (LQ20F050010); 浙江省教育厅一般项目 (Y201942186); 浙江省自然科学基金 (LY20F010001); 浙江省重点研发计划项目 2020C03094; 国家自然科学基金青年科学基金 (61801429)

作者简介: 徐璐 (1988-), 男, 讲师, 博士, 主要从事光子计数成像激光雷达、三维点云图像处理方面的研究工作。Email: xlhit@ 126.com

通讯作者: 吴龙 (1978-), 男, 讲师, 博士, 主要从事成像激光雷达方面的研究。Email: wulong@zstu.edu.cn

0 Introduction

Geiger-mode avalanche photodiode (Gm-APD) is widely used in the 3D imaging lidar system to detect weak signals because of their single-photon sensitivity and picosecond magnitude time precision [1–3]. Gm-APD cannot directly obtain the strength information because it can only respond to the presence or absence of the signal. The signal output of the detector is 1 or 0, which is a digital detection technology [4–6]. Two methods are usually used to indirectly obtain the signal strength information. The first method is to use the photon counts under accumulated detection to represent the intensity information of the target [7–8]. However, since the output, photon counts, and input, photoelectron number, are not a linear relationship in Gm-APD, this method is an approximate method [9]. The other method is to obtain the number of signal photoelectrons according to the Poisson probability model of Gm-APD to represent the intensity [10], which is more accurate.

Gm-APD has first photon bias effect [11]. This phenomenon is due to the dead time (almost 50 ns) and nonlinear model of Poisson probability response of Gm-APD. For a pulsed accumulated Gm-APD photon counting lidar, the input of the probability response model of Gm-APD is signal photoelectron distribution histogram (SPDH), while the output is photon counting distribution histogram (PCDH). These two diagrams are different, which is caused by the first photon bias effect. Thus, the effect will cause the range walk error in photon counting lidar [12].

The range walk error depends on the intensity and waveform of receiving signal. It will cause deterioration with signal enhancing and pulse width broadening [12]. The reflectivity of the target is always not uniform. The fluctuation in the number of signal photoelectrons reflected from the target can cause different range walk errors, which will generate the distortion of depth image of the target. The range walk error needs to be restrained.

Two methods were proposed to restrain the range walk error by Oh *et al* [13] and He *et al* [14], respectively. But these two methods both need priori models. Later, He *et al* presented a real-time restraint method by unequally intensity-dividing the echo pulses into two Gm-APDs. They censored the anomalous pixels in the matrix to obtain the accurate depth image [15]. The above studies researched on the narrow pulses, about 100 ps pulse width. Previously, we proposed two methods to restrain the range walk error without priori models using a 6 ns width wide pulse[12, 16], which will be used in this paper.

In this paper, two methods to restrain the range walk error are presented and verified by experiments. A high precision of 3D image of the target is obtained.

1 Theoretical analysis

According to the Poisson probability response model of a Gm-APD, the avalanche probability of the *i*-th time bin with discrete time bins is presented as [17]

$$P(i)=\{1-\exp[-N_{\mathrm{sn}}(i)]\}\exp\left[-\sum_{j=i-d}^{i-1}N_{\mathrm{sn}}(j)\right] \tag{1}$$

where $N_{\mathrm{sn}}(i)=N_{\mathrm{s}}(i)+N_{\mathrm{n}}(i)$, $N_{\mathrm{s}}(i)$ is the number of signal photoelectrons in the *i*-th time bin, $N_{\mathrm{n}}(i)$is the number of noise photoelectrons in the *i*-th time bin, and *d* is the dead time of the Gm-APD.

In a time-of-arrival histogram built up over many laser pulses, the avalanche probability of a Gm-APD can be obtained by the following formula:

$$P(i)=\frac{K(i)}{M} \tag{2}$$

where $K(i)$ is the number of photon counts of the Gm-APD in the *i*-th time bin, and *M* is the total number of detections.

Substitute Eq. (2) to Eq. (1), we can get

$$K(i)=M\{1-\exp[-N_{\mathrm{sn}}(i)]\}\exp\left[-\sum_{j=i-d}^{i-1}N_{\mathrm{sn}}(j)\right] \tag{3}$$

Let $K(i)$ go through the all time bins, it is the SPDH of Gm-APD in the experiment.

In our previous research work [12], we proposed an echo signal restoration method to obtain SPDH from the

PCDH of Gm-APD. The SPDH is obtained as

$$N_s'(i) = -\ln\left\{1 - \frac{K(i)}{M}\exp\left[\sum_{j=i-d}^{i-1} N_s(j) + \sum_{j=i-d}^{i-1} N_n(j)\right]\right\} - N_n(i) \tag{4}$$

Calculating the sum of all signal photoelectrons in the signal interval, from T_1 to T_m, the intensity information of the target can be obtained by

$$I = \sum_{i=T}^{T_m} N_s'(i) \tag{5}$$

In the traditional time-of-flight Gm-APD lidar, there exists range walk error between the distances of measured value and truth value, which is caused by the first photon bias effect of Gm-APD. It will cause deterioration with signal enhancing and pulse width broadening. There are two methods for traditional pulse peak ranging [18] and center-of-mass algorithm ranging [19]. Based on these two pulse ranging methods, we will propose two methods to restrain the range walk error.

The first method is signal restoration & Gaussian functions fitting method. According to the SPDH corresponding to the measurements, it is found that the function with the sum of two Gaussian curves fits well. The fitting curve shows a central peak shape and meets the following equation,

$$N_s'(i) = A_1\exp\left[\frac{-(i-T_1)^2}{B_1^2}\right] + A_2\exp\left[\frac{-(i-T_2)^2}{B_2^2}\right] \tag{6}$$

where A_1, T_1, B_1, A_2, T_2, and B_2 are constants obtained by MATLAB. The peak position of the fitting curve, T, is the time-of-flight of the laser pulse. The distance information of the target can be obtained by

$$R' = \frac{c}{2}\times T \tag{7}$$

where $c = 3\times10^8$ m/s.

The second method is signal restoration & center-of-mass algorithm method. The center-of-mass algorithm method is used on the SPDH. The distance information of the target can be obtained by

$$R'' = \frac{c\Delta t}{2}\frac{\sum_{i=T}^{T_m} iN_s'(i)}{\sum_{i=T}^{T_m} N_s'(i)} \tag{8}$$

Both the two methods can effectively suppress the range walk error to obtain high-precision intensity and distance information of the target.

2 Experimental analysis

2.1 Experimental system design

Figure 1 shows the Gm-APD lidar system. Figure 1(a) shows the schematic diagram of the designed Gm-APD lidar. The signal generator gives a trigger signal to the laser to emit a pulse at wavelength of 1 064 nm, which is transformed into 532 nm by a frequency doubling crystal (FDC). The laser is divided into two beams using a beam splitter (BS). One beam is collected by a high-speed PIN detector to trigger the DPC-230 photon correlator card to record the start time, and the other beam illuminates the target after an *X*-*Y* scanning system. The scattered light returned from the target is collected by the receiving system. Then it is decayed to photon level by the attenuators. Lastly, the photon signal is detected by a Gm-

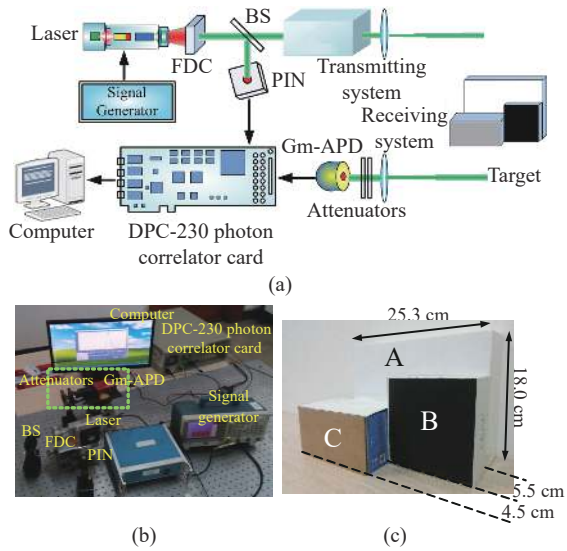

Fig.1 Gm-APD lidar system. (a) Schematic of the Gm-APD lidar (FDC: frequency doubling crystal, BS: beam splitter, PIN: high speed PIN detector, Gm-APD: Gm-APD detector module); (b) Photograph of the lidar system; (c) Photograph of the target

APD module. The Gm-APD module outputs a Transistor Transistor Logic (TTL) signal to stop the DPC-230 card. The PCDH is obtained after a number of detections.

The photograph of the indoor confirmatory lidar system is shown in Fig.1(b). In order to simulate a strong sunlight background, the narrowband filer is not used. Moreover, ten fluorescent lamps are utilized to achieve a strong background noise of 1.49×10^7 Hz, which is measured without any attenuators.

Figure 1(c) shows the targets (A, B, and C) covered with different reflectivity materials. The distances of the three targets are 525 cm, 519.5 cm, and 515 cm, respectively. The size of target A is 25.3 cm×18 cm. The diameter of the laser spot illuminated on the target is 5 mm, and the scanning points are 30×46. Table 1 shows the performance parameters of the devices in the experiment.

Tab.1 Performance parameters of the devices in the experiment

Devices	Performance parameters
Semiconductor laser	Pulse width 6 ns, wavelength 1 064 nm, repetition frequency 2 kHz Work wavelength of the lidar 532 nm
Receiving telescope	Aperture diameter 23 mm, field of view<100 mrad
Gm-APD module	COUNT-100C, Laser Components GmbH. dead time 45 ns, photon detection efficiency 70%@532 nm, dark count rate 100 Hz, length of TTL output pulse 15 ns, high level 3 V, temporal jittering 1 000 ps, maximum count rate 20 MHz
Photon correlator card	DPC-230, Becker & Hickl GmbH. Time duration of time-bin 164 ps, operating mode “Multicaler”, collection time 60 s, total detection number 1.2×10^5

2.2 Experimental results and analysis

The PCDH of the Gm-APD is completely submerged in the noise and the signal cannot be identified under the strong background noise of 1.49×10^7 Hz, as shown in Fig.2(a). We use 50 dB attenuators to enhance the signal-to-noise ratio. The signal completely submerged in the noise is perfectly captured, as shown in Fig.2(b). This is a phenomenon peculiar to the Gm-APD.

Figure 3 shows the logical diagram of the two methods to restrain the range walk error. We directly capture the PCDH, output of Gm-APD, acquired by DPC-230 photon correlator card. The PCDH is expressed as Eq.(3), which is a recursive formula. We need go through the signal time bins, from T_1 to T_m. Then, signal restoration method is used to obtain SPDH from the PCDH. It is calculated by Eq.(4). There is an offset between SPDH and PCDH. They do not coincide, which is the range walk error. This is detailed explained in our previous work of Ref. [12]. We need find the distance information from the SPDH. The first method uses a sum of two Gaussian functions to fit the SPDH, and finds the peak position of the curve to calculate the distance. The intensity information is calculated by the area of the fitting curve, and the distance information is calculated by Eq.(7). The second method uses the center-of-mass algorithm method on the SPDH to calculate the distance. The intensity information is calculated by Eq.(5), and the distance information is calculated by Eq.(8).

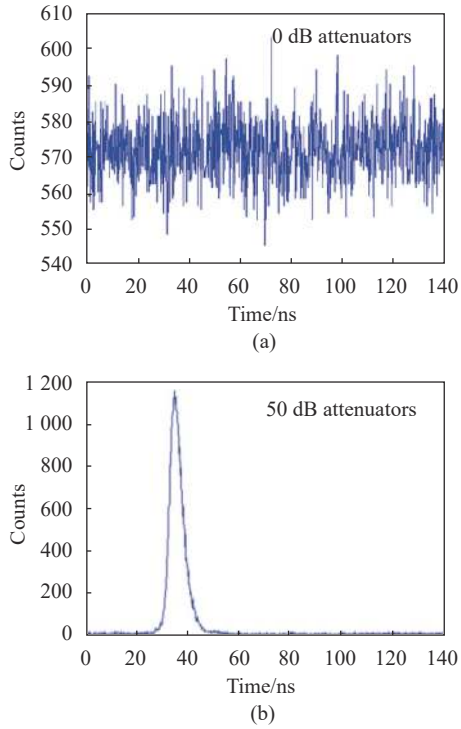

Fig.2 PCDH of target A with different attenuators. (a) 0 dB attenuators; (b) 50 dB attenuators

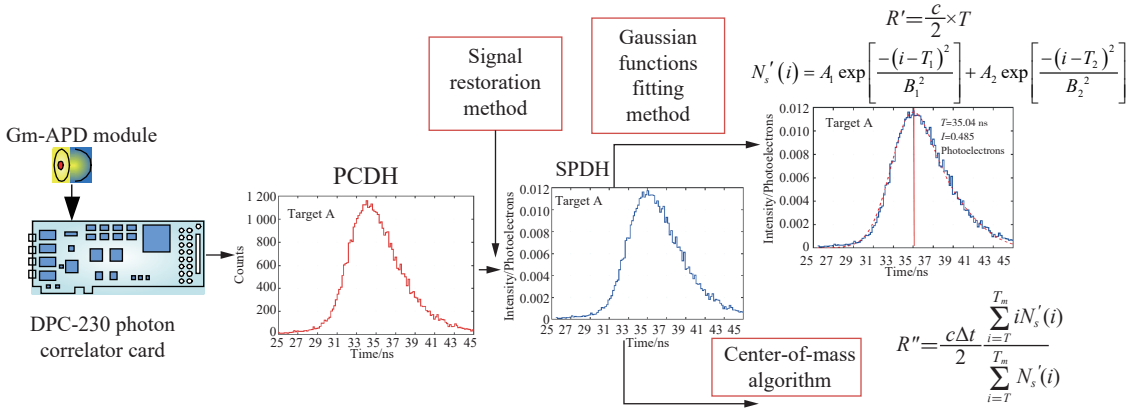

Fig.3 Logical diagram of the two methods to restrain range walk error

The relative accuracy of intensity is calculated by

$$\frac{\sigma_I}{\bar{I}}=\frac{\sqrt{\frac{1}{N}\sum_{i=1}^{N}\left(I_i-\bar{I}\right)^2}}{\bar{I}} \tag{9}$$

where N is the pixel number of a target, I_i is the measurement intensity of the i-th pixel, and $\bar{I}$is the average measured intensity of a target.

The range precision is calculated by

$$\sigma_R=\sqrt{\frac{1}{N}\sum_{i=1}^{N}\left(R_i-\bar{R}\right)^2} \tag{10}$$

where R_i is the measurement distance of the i-th pixel, obtained by Eq.(7) or Eq. (8), and $\bar{R}$ is the average measured intensity of a target.

Figure 4 shows the experimental imaging results of signal restoration & Gaussian functions fitting method. Fig.4(a) shows the depth image with a color map corresponding to the distance using traditional pulse peak ranging method. It lacks intensity information of the target. The measured mean distance of the target A, B, and C are 517.6 cm, 515.9 cm, and 509.8 cm, respectively. The corresponding range walk errors are −7.4 cm, −3.6 cm, and −5.2 cm, respectively. The range walk error effect is very serious. We can only find two distance values from the distance distribution histogram of Fig.4(a), as shown in Fig.4(c). Figure 4(b) shows the 3D plot of depth image with a color map corresponding to the intensity using the signal restoration & Gaussian functions fitting method. We get the depth-intensity 3D merged image. The measured mean distance of the target A, B, and C are 525.6 cm, 519.7 cm, and 514.9 cm, respectively. The corresponding range walk errors are +0.6 cm, +0.2 cm, and −0.1 cm, respectively. The restraint of range walk error is effective. The measured mean intensity of the target A, B, and C are 0.492, 0.231, and 0.314 photo-electrons. The relative accuracy of intensity measurement, obtained by Eq. (9), is less than 3%. We can observe three distance values from the distance distribution histogram of Fig. 4(b), as shown in Fig. 4(d). However, there are some overlap between them. The range precision, obtained by Eq. (10), is 1.2 cm.

Figure 5 shows the experimental imaging results of signal restoration & center-of-mass algorithm method. Figure 5(a) shows the depth image with a color map corresponding to the distance using traditional center-of-mass algorithm method. It lacks intensity information of the target as well. The measured mean distance of the target A, B, and C are 519.4 cm, 517.4 cm, and 511.0 cm, respectively. The corresponding range walk errors are −5.6 cm, −2.1 cm, and −4.0 cm, respectively. The range walk error effect is very serious. We can find three distance values from the distance distribution histogram of Fig. 5(a), as shown in Fig. 5(c). However, there are some overlap between them. Figure 5(b) shows the 3D plot of depth image with a color map corresponding to the intensity using the signal restoration & center-of-mass algorithm method. We get the depth-intensity 3D merged

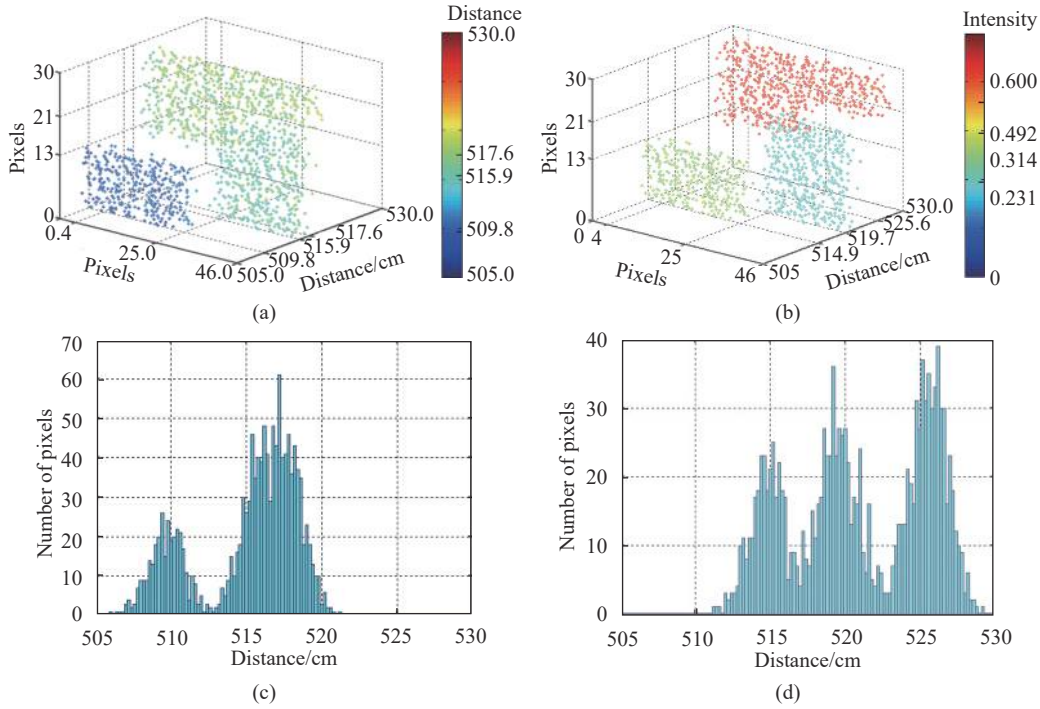

Fig.4 Experimental imaging results of Gaussian functions fitting method. (a) Depth image with a color map corresponding to the distance using the traditional pulse peak ranging method. (b) 3D plot of depth image with a color map corresponding to the intensity using the signal restoration & Gaussian functions fitting method. (c) Distance distribution histogram of Fig. 3(a). (d) Distance distribution histogram of Fig. 3(b)

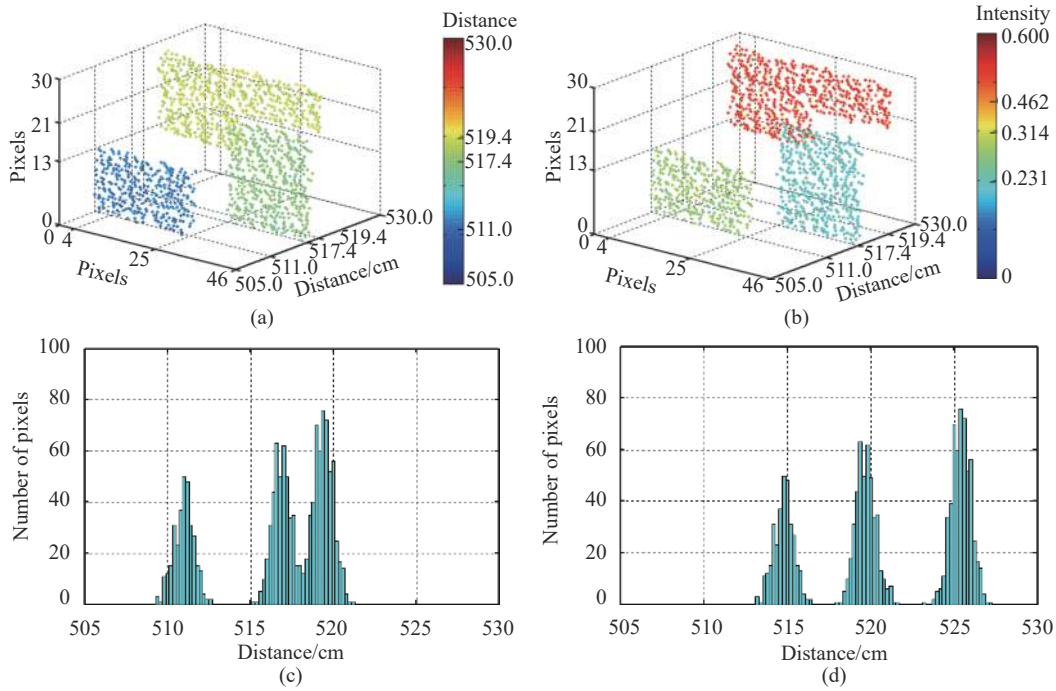

Fig.5 Experimental imaging results of center-of-mass algorithm method. (a) Depth image with a color map corresponding to the distance using the traditional center-of-mass algorithm method. (b) 3D plot of depth image with a color map corresponding to the intensity using the signal restoration & center-of-mass algorithm method. (c) Distance distribution histogram of Fig. 4(a). (d) Distance distribution histogram of Fig. 4(b)

image. The measured mean distance of the target A, B, and C are 525.4 cm, 519.7 cm, and 514.8 cm, respectively. The corresponding range walk errors are +0.4 cm, +0.2 cm, and −0.2 cm, respectively. The restraint of range walk error is effective. The measured mean intensity of the target A, B, and C are 0.492, 0.231, and 0.314 photo-electrons. The relative accuracy of intensity measurement, obtained by Eq. (9), is less than 3%. We can clearly observe three distance values from the distance distribution histogram of Fig. 5(b), as shown in Fig. 5(d). There is no overlap between each other. The range precision, obtained by Eq. (10), is 0.6 cm, which is high enough.

The signal restoration & Gaussian functions fitting method, and the signal restoration & center-of-mass algorithm method both can effectively suppress the range walk error and obtain high-precision depth-intensity 3D merged image of the target. However, the signal restoration & Gaussian functions fitting method is inconvenient. The target distance is determined by the peak position of the fitting curve, which is the sum of two Gaussians. Nevertheless, the small region near the peak is smooth and nearly straight line in some cases. This condition excessively increases the uncertainly of the peak position. Therefore, the first method has lower range precision of 1.2 cm. Fortunately, the weighted method can solve this problem. The signal restoration & center-of-mass algorithm method is more convenient and more stable. The restraining effect on the range walk error is very good. The second method has higher range precision of 0.6 cm.

3 Conclusion

Due to the first photon bias effect of Gm-APD, there exists range walk error in the Gm-APD lidar. It will cause deterioration with signal enhancing and pulse width broadening. The fluctuation in the number of signal photoelectrons reflected from the target can cause different range walk errors, which will generate the distortion of depth image of the target. In this paper, two methods to restrain the range walk error are presented and verified by experiments. A high precision of 3D image of the target is obtained, respectively.

Firstly, we theoretically analyze the principle of range walk error in Gm-APD lidar. Secondly, we propose a signal restoration method to obtain SPDH from the PCDH, which can also obtain the intensity of the target. Gaussian functions fitting method and center-of-mass algorithm method are used to capture the distance from the SPDH, respectively. Finally, we verified the two methods by experiments. The relative accuracy of intensity measurement of the two methods are both less than 3%. The first method has lower range precision of 1.2 cm. The second method has higher range precision of 0.6 cm.

Both the two methods use data processing methods to improve the range precision. In order to further improve the range precision, devices with higher performance parameters can also be used. For example, using a Gm-APD module with lower time jitter, a photon counting board with higher time resolution, and a laser with a more stable pulse waveform. However, these will inevitably cause much more cost of system manufacturing. The main factor that limits the range precision is the time jitter of the Gm-APD module. It is about 1 000 ps in these experiments. It can be replaced by a Gm-APD module with a time jitter of several hundred ps.

References:

[1] Steinvall O, Sjöqvist L, Henriksson M. Photon counting ladar work at FOI, Sweden[C]// Proc SPIE, 2012, 8375: 83750C.

[2] Luo L, Wu C, Lin J, et al. Time-domain denoising based on photon-counting LiDAR [J]. ***Optics and Precision Engineering***, 2018, 26(5): 1175-1180. (in Chinese)

[3] Xu L, Zhang Y, Zhang Y, et al. Four Gm-APDs photon counting imaging lidar to improve detection performances [J]. ***Infrared and Laser Engineering***, 2015, 44(9): 2583-2587. (in Chinese)

[4] Albota M A, Aull B F, Fouche D G, et al. Three-dimensional imaging laser radars with Geiger-mode avalanche photodiode

arrays [J]. ***Lincoln Laboratory Journal***, 2002, 13(2): 351-370.

[5] Cho P, Anderson H, Hatch R, et al. Real-time 3D ladar imaging [J]. ***Lincoln Laboratory Journal***, 2006, 16(1): 147-164.

[6] Ma L, Lu W, Jiang P, et al. Research on 3D range reconstruction algorithm of Gm-APD lidar based on matched filter [J]. ***Infrared and Laser Engineering***, 2020, 49(2): 020500. (in Chinese)

[7] Buller G S, Krichel N J, McCarthy A, et al. Kilometer range depth imaging using time-correlated single-photon counting[C]// Proc SPIE, 2011, 8155: 81551I.

[8] Lussana R, Villa F, Dalla Mora A, et al. Enhanced single-photon time-of-flight 3D ranging [J]. ***Optics Express***, 2015, 23(19): 24962-24973.

[9] Liu D, Sun J, Jiang P, et al. GM-APD lidar range image reconstruction based on neighborhood KDE [J]. ***Infrared and Laser Engineering***, 2019, 48(6): 630001. (in Chinese)

[10] Kirmani A, Venkatraman D, Shin D, et al. First-photon imaging [J]. ***Science***, 2014, 343(6166): 58-61.

[11] Barton-Grimley R A, Thayer J P, Hayman M. Nonlinear target count rate estimation in single-photon lidar due to first photon bias [J]. ***Optics Letters***, 2019, 44(5): 1249-1252.

[12] Xu L, Zhang Y, Zhang Y, et al. Restraint of range walk error in a Geiger-mode avalanche photodiode lidar to acquire high-precision depth and intensity information [J]. ***Applied Optics***, 2016, 55(7): 1683-1687.

[13] Oh M S, Kong H J, Kim T H, et al. Reduction of range walk error in direct detection laser radar using a Geiger mode avalanche photodiode [J]. ***Optics Communications***, 2010, 283(2): 304-308.

[14] He W, Sima B, Chen Y, et al. A correction method for range walk error in photon counting 3D imaging LIDAR [J]. ***Optics Communications***, 2013, 308: 211-217.

[15] Ye L, Gu G, He W, et al. A real-time restraint method for range walk error in 3-D imaging lidar via dual detection [J]. ***IEEE Photonics Journal***, 2018, 10(2): 1-9.

[16] Xu L, Zhang Y, Zhang Y, et al. Signal restoration method for restraining the range walk error of Geiger-mode avalanche photodiode lidar in acquiring a merged three-dimensional image [J]. ***Applied Optics***, 2017, 56(11): 3059-3063.

[17] Johnson S, Gatt P, Nichols T. Analysis of Geiger-mode APD laser radars[C]// Proc SPIE, 2003, 5086: 359-368.

[18] Wu Y, Zhou M, Zhao Q, et al. Threshold-peak dual-channel time discrimination method for pulse laser ranging [J]. ***Infrared and Laser Engineering***, 2019, 48(6): 0606002. (in Chinese)

[19] Busck J, Heiselberg H. Gated viewing and high-accuracy three-dimensional laser radar [J]. ***Applied Optics***, 2004, 43(24): 4705-4710.